◆ Human Brain Mapping 35:5532–5549 (2014) ◆

Characteristics of Canonical Intrinsic Connectivity Networks Across Tasks and Monozygotic Twin Pairs

Craig A. Moodie,[1] Krista M. Wisner,[2] and Angus W. MacDonald III[1,2,3]*

[1]*Department of Neuroscience, University of Minnesota Medical School, Minneapolis, Minnesota*
[2]*Department of Psychology, University of Minnesota, Minneapolis, Minnesota*
[3]*Department of Psychiatry, University of Minnesota Medical School, Minneapolis, Minnesota*

Abstract: Intrinsic connectivity networks (ICNs) are becoming more prominent in the analyses of in vivo brain activity as the field of neurometrics has revealed their importance for augmenting traditional cognitive neuroscience approaches. Consequently, tools that assess the coherence, or connectivity, and morphology of ICNs are being developed to support inferences and assumptions about the dynamics of the brain. Recently, we reported trait-like profiles of ICNs showing reliability over time and reproducibility across different contexts. This study further examined the trait-like and familial nature of ICNs by utilizing two divergent task paradigms in twins. The study aimed to identify stable network phenotypes that exhibited sensitivity to individual differences and external perturbations in task demands. Analogous ICNs were detected in each task and these ICNs showed consistency in morphology and intranetwork coherence across tasks, whereas the ICN timecourse dynamics showed sensitivity to task demands. Specifically, the timecourse of an arm/hand sensorimotor network showed the strongest correlation with the timeline of a hand imitation task, and the timecourse of a language-processing network showed the strongest temporal association with a verb generation task. The area V1/simple visual stimuli network exhibited the most consistency in morphology, coherence, and timecourse dynamics within and across tasks. Similarly, this network exhibited familiality in all three domains as well. Hence, this experiment is a proof of principle that the morphology and coherence of ICNs can be consistent both within and across tasks, that ICN timecourses can be differentially and meaningfully modulated by a task, and that these domains can exhibit familiality. *Hum Brain Mapp 35:5532–5549, 2014.* © **2014 Wiley Periodicals, Inc.**

Key words: functional connectivity; twin study; intrinsic connectivity networks; neurometrics; independent components analysis; heritability; task; consistency

INTRODUCTION

The burgeoning field of functional connectivity magnetic resonance imaging (fcMRI) has shown marked interest in developing our understanding of brain activity from the perspectives of both functional specialization and integration [Behrens and Sporns, 2011; Smith, 2012]. Several methods have been developed for assembling the voxelwise fcMRI signals across the brain to form networks based on their functional covariation, that is, their intrinsic

Additional Supporting Information may be found in the online version of this article.

*Correspondence to: Angus MacDonald, Department of Psychology, University of Minnesota, 75 E River Road, Minneapolis, Minnesota, USA. E-mail: angus@umn.edu

Received for publication 7 October 2013; Revised 6 May 2014; Accepted 11 June 2014.

DOI: 10.1002/hbm.22568
Published online 1 July 2014 in Wiley Online Library (wileyonlinelibrary.com).

connectivity or coherence [Beckmann and Smith, 2004; Calhoun and Adali, 2001; Fox and Raichle, 2007; Mckeown et al., 1998], and the existence of these networks has been corroborated using other techniques such as magnetoencephalography and electroencephalography [Calhoun et al., 2009; Pasquale et al., 2012]. These findings show that intrinsic connectivity networks (ICNs), observed using fcMRI techniques, can be moderately reliable nonartifactual networks that correspond in their location and behavioral significance to well-established areas and canonical brain processes such as vision, motor control, and executive function [Behrens and Sporns, 2011; Deco et al., 2009; Lahaye et al., 2003; Meier et al., 2012; Repovš and Barch, 2012; Smith, 2012; Snyder and Raichle, 2012]. For instance, an independent component analysis (ICA) of activation maps from the numerous behavioral paradigms in the BrainMap database generated activation networks that were morphologically similar to the ICNs extracted from resting state scans [Smith et al., 2009]. Furthermore, functional associations were derived for the BrainMap networks as a guide for tests of the reverse inference of data-driven ICNs, such as this study [Laird et al., 2011].

Other groups have been interested in how ICNs may be useful for studying individual differences and/or the biological basis of psychopathology [Fornito and Bullmore, 2012; Guo et al., 2012; Van Dijk et al., 2010]. However, it is important to first consider whether ICNs possess a neurometric profile necessary for these purposes. Some findings suggest that ICNs are not only reproducible and replicable at a group level, but that their test–retest reliability is also strong at the individual level [Anderson et al., 2011; Chou et al., 2012; Shehzad et al., 2009; Thomason et al., 2011; Zuo et al., 2010]. Hence, with some caveats, the network profiles appear to be reliable individual difference traits [Poppe et al., 2013; Wisner et al., 2013]. These findings are consistent with the studies showing that ICNs appear to be present irrespective of task demands or cognitive states, including rest and sedation [Arbabshirani et al., 2012; Biswal et al., 2010; Calhoun and Adali, 2001; Calhoun et al., 2001, 2008; Deco et al., 2011; Greicius et al., 2008; Li et al., 2012; Poppe et al., 2013; Sämann et al., 2011; Smith et al., 2009]. To further examine the trait-like nature of ICNs, this study builds on these previous neurometric findings by examining (1) whether individual differences in canonical ICNs are consistent within tasks, and (2) across tasks within participants, (3) the manner in which network consistency may vary with task demands and engagement, and (4) to what extent these individual differences might be similar across monozygotic twin pairs.

The question of the consistency of ICNs, both within task and across different tasks, has both theoretic and practical significance. Two fundamental questions about the nature of ICNs that remain are whether they are stable over time and whether they reflect structural–functional "priors" or, in effect, networks in a reserve state, waiting to be activated by appropriate cognitive demands [Deco et al., 2011]. A great deal of work has preceded under the unexamined assumption that individual differences in the profiles of "reserve" ICNs anticipate individual differences in ICNs when they are relevant to brain functioning. There is indirect evidence that resting state (reserve) ICNs have a similar structure to task-related networks [Calhoun et al., 2008; Kristo et al., 2012; Smith et al., 2009], and thus supporting this hypothesis and the potential for predictive capacity across task demands. However, there is no direct evidence, to date, that the characteristics of a complement of data-driven ICNs can describe traits across the brain and across circumstances.

One approach to this question is to examine whether phenotypes exhibited by ICNs during one task are predictive of phenotypes in a different task. It should then be possible to determine the degree to which each ICN, observed in each behavioral assay, is involved with that task and how its characteristics change with respect to changing task demands. By doing so, this approach can also be used to validate the functional associations of canonical networks recently described in a meta-analysis of activation studies [Laird et al., 2011]. Additionally, by using functional localizer tasks, which are paradigms that were designed to drive activation reflecting specific cognitive processes, this study also examined whether ICNs were detected equally well across paradigms, enabling a test of convergence and divergence of ICNs across cognitively driven brain states.

Another consideration when establishing new metrics is the extent to which they are influenced by familial versus nonshared environmental factors. Familiality, which includes both heritable and shared environment influences, can be examined using twin study designs. Heritable influences have been reported on cognitive–behavioral phenotypes as diverse as intelligence, memory, and personality, as well as psychiatric syndromes such as schizophrenia, depression, and autism [Blokland et al., 2011; Hallmayer et al., 2011; Jang et al., 2011; Molloy et al., 2001; Tost et al., 2011]. It is, therefore, not surprising that twin studies have also found that the development, structural architecture, cortical profile, and functional activity of the brain also show large heritable components [Ambrosius et al., 2008; Belmonte and Carper, 2006; Blokland et al., 2008; Borgwardt et al., 2010; Brun et al., 2009; Chen et al., 2012; Chiang et al., 2011; Deco et al., 2011; Duarte-Carvajalino et al., 2012; Glahn et al., 2010; Hagmann et al., 2010; Honey et al., 2010; Jahanshad et al., 2010; Matthews et al., 2007; Meyer-Lindenberg, 2009; Munn et al., 2007; Rimol et al., 2010; Tarokh et al., 2011; Yang et al., 2012].

These findings support the investigation of the heritability of ICNs and, hence, population variance in ICNs should be related to population variance in genes. Monozygotic twin designs provide a division between nonshared environmental influences and familial influences, which include shared environmental and additive genetic factors, of which the primary source of familial variance is genetic [Belmonte and Carper, 2006; Blokland et al., 2011; Matthews et al., 2007]. As a result, in this study we

assessed the familial, and therefore primarily genetic, contribution to the characteristics of ICA-derived ICNs by using a monozygotic twin sample to examine the consistency of ICN measurements in two paradigms. Hence, this proof of principle approach allowed us to investigate the extent to which ICNs could be viewed as traits, and whether ICNs that were trait-like were also familial in this sample.

METHODS

Participants

Twenty-six pairs of right-handed monozygotic twins (13 female pairs, 13 male pairs, mean age 25.02 ± 5.36 SD; range, 19–34) were recruited for this study from a larger sample of 1,388 twin pairs from the Minnesota Twin Registry. All twins were prescreened for pre-existing medical, neurological, or psychiatric conditions and personality characteristics relevant to a decision-making task not further reported here. All participants were given written, informed consent before participating in the study, and the Institutional Review Board of the University of Minnesota approved all experiments. Five twin pairs were excluded from the analysis owing to one member not having the entire complement of scans, or technical problems during the scanning session.

Hand Imitation and Verb Generation Tasks

Each participant was trained prior to the start of the experiment and all participants performed two behavioral tasks, *Hand Imitation* (HI) and *Verb Generation* (VG), that were designed to drive brain activity in a specific way (functional localizers). The tasks included a 6-min run each of HI and VG, from the International Consortium on Brain Mapping (ICBM) test battery, within a single scanning session [Mazziotta et al., 2001, 2009]. HI and VG had an identical block design and subtraction condition: six 30″ experimental blocks were interspersed with 30″ control blocks in which participants performed an arrow-monitoring activity. The two tasks had the same Nyquist frequency (0.17 Hz), as well as the same trial frequency (0.5 Hz) and the total experimental time for each task was 6 min. Within the experimental blocks for both tasks, there were 15 analogous 2-s trial periods. For HI, participants imitated a novel hand position during the 2-s trial period. For VG, a drawing of a familiar object was flashed on-screen for a 500-ms presentation period, followed by a 1.5-s response window for participants to silently generate a verb associated with the picture without actually moving their lips. The control task involved fixating on a central cross, after which an arrow would appear on the screen pointing in one of the four directions. Participants pressed a button with their left thumb when the arrow was pointing left.

MR Acquisition and Preprocessing

All data were collected on a 3T Siemens Trio MRI scanner using a 6-channel transmit, 12-channel receive head coil. One identical whole-brain functional scan each was collected for the HI and VG tasks (EPI; repetition time = 2,000 ms, echo time = 28 ms; flip angle = 90°; voxel size = 3.5 × 3.5 × 3.5 mm; matrix size = 64 × 64, axial orientation; number of slices = 34, slice thickness = 3.5 mm, spacing between slices = 3.5 mm, interleaved slice acquisition). In addition, a high-definition structural T1-weighted image (MPRAGE) was also collected per participant.

All MRI data were preprocessed and analyzed using the FMRIB FSL 4.1.8 software package (http://www.fmrib.ox.ac.uk/fsl). Prestatistical processing steps included high-pass temporal filtering (70 s = 0.014 Hz), motion correction via the MCFLIRT linear registration algorithm [Jenkinson et al., 2002], BET brain extraction, interleaved slice-timing correction, and spatial smoothing with a 5-mm full-width half-maximum Gaussian kernel. For each participant, the functional scans were registered to their high-resolution T1 images and then to the 2-mm standard-space MNI brain using nonlinear algorithms with a 2-mm resampling resolution and 10-mm warp kernel [Andersson et al., 2007].

FMRI Data Analysis

Intrinsic connectivity network generation

To generate reliable data-driven networks that reflected functional regions in the brain, the EPI scans for both tasks were processed via temporal concatenation group independent component analyses using FSL's MELODIC ICA toolkit [Beckmann and Smith, 2004]. The algorithms were constrained using a dimensionality of thirty (30) components and all components that clearly did not reflect physiologically relevant BOLD-dependent signal were excluded from subsequent analyses. The remaining nonartifactual components were subsequently identified as ICNs [Beckmann, 2012; Calhoun et al., 2009; Zuo et al., 2010]. Given that roughly one-third of the components tended to be artifactual, 30 components were the optimal dimensionality to match the nonartifactual components with the 20 BrainMap networks derived by Laird et al. (2011) and utilize said networks for reverse inference [Bhaganagarapu et al., 2013; Ray et al., 2013].

Additionally, to avoid artificially inflating correlations between tasks and twins, and to allow for cross-validation analyses, group-level ICNs were generated separately for each task (HI, then VG) and, within each task, for two subgroups containing one member of each twin pair (all twin 1s and then all twin 2s). Owing to possible participant scan concatenation and initial random value effects, a participant-order permutation and combination procedure was performed, which involved running multiple MELODICs and deriving a set of meta-level ICNs,

reflecting consistent components across the permutations [Wisner et al., 2013]. Once the meta-level ICNs were obtained, the FSL spatiotemporal regression algorithm was used to generate participant-level network spatial maps and timecourses for the ICNs derived from each task (http://www.fmrib.ox.ac.uk/analysis/dualreg).

ICN morphology analyses

When assessing ICN morphology, all 3D spatial maps were thresholded using a conservative threshold ($z = 6$) to limit the maps to only voxels that were highly significant and contributed most to the ICN morphology [Wisner et al., 2013]. Spearman rank correlations and Dice similarity indices were then calculated in each set of comparisons. Given the relationship between the Dice similarity index and Cohen's kappa, a Dice of $s \geq 0.4$ (max = 1.0) represented fair to good overlap [Agresti, 2013; Banerjee et al., 2012]. These metrics were first computed between thresholded group-level ICNs ($z = 6$) from the HI and VG tasks and the ICNs were then displayed at higher thresholds during 3D rendering to simplify the maps for viewing. Second, these metrics were computed between the group-level ICNs and the canonical BrainMap networks [Laird et al., 2011] at the standard threshold ($z = 6$) for reverse inference testing. ICNs with good Dice similarity ($s > 0.4$) for these comparisons were considered to have a reasonable amount of overlap with the BrainMap networks. Hence, this test functioned as one external validation for the ICNs generated from the two distinct functional scans.

Next, similar procedures were completed at the participant level. Participant-specific spatial maps of the ICNs were thresholded as mentioned above ($z = 6$) and spatial correlations were performed between each twin and his or her co-twin, as well as every other participant in the study for each ICN. Heatmap matrices were generated per ICN to visualize these spatial correlations and to determine if twin pair correlation scores were distinguishable from the correlation scores for the entire sample. All ICN correlation matrices were averaged to produce a final heatmap with a value for the average spatial correlation across all ICNs for all twins. A *t*-test contrasting the mean ICN correlation scores for twin pairs versus scores for the pairs of unrelated participants was performed. Subsequently, a nonparametric permutation test [Hothorn and Hornik, 2011], employing random reassignment of twin pair membership, was completed to validate the results of the *t*-test using a method in which no assumptions would be violated by genetic covariance.

Finally, spatial correlation analyses that included Spearman and Dice coefficient tests were performed between the participant-level ICN spatial maps and the spatial maps of the group level ICNs. This was done to determine the extent to which each individual's spatial maps conformed to the group ICN spatial maps. For the spatial familiality metric, an intraclass correlation (ICC) of the Dice similarity coefficients within twin pairs was calculated per ICN to ascertain which ICNs exhibited familiality.

ICN coherence analyses

The intranetwork coherence of an ICN is an estimate of how well the timecourses of voxels in a participant-level ICN fit the group-level timecourse vector and, hence, is a measure of the intrinsic connectivity strength of that network. To obtain an estimate of the familiality of intranetwork coherence, both voxelwise and network-level mean ICC's were computed using an image data (nifti file) algorithm and the ICC package in R^{TM} from CRAN (http://cran.r-project.org/), respectively [Revelle, 2011]. First, the participant-level network spatial maps were masked using a binarized image of a task-specific group-level ICN map that had been prethresholded ($z = 6$). Voxelwise ICC's were then calculated across twins using the FMRIB fslmaths algorithm, and the mean of the ICC values across the voxels within the mask was recorded per ICN, per participant (Supporting Information Methods). Second, the network-level mean coherence score for each thresholded ICN spatial map was calculated per participant using the fslstats tool (Supporting Information Methods). R^{TM} was then used to calculate ICC's of the resulting average network coherence coefficients across twins for all ICNs, within each task separately, and this was used as the basis of the coherence familiality metric.

ICN timecourse analyses

To examine the relationship between the ICNs and the respective task designs, Pearson correlations were performed between the timecourse of each participant-level ICN and the convolved task hemodynamic response function (HRF) design matrix for that individual. Hence, the relationship between the timecourse of each ICN and the HRF associated with task demands could be computed per individual. This consequently revealed the extent to which each network was engaged by the task for both the HI and the VG paradigms. For each task, these correlations (after *z*-transformation) were averaged across all participants per ICN and the mean correlations were used as the basis for determining the degree to which each ICN was involved with the task in the "relationship to task" metric. Additionally, *z*-transformed correlation scores were correlated within twin pairs for the task HRF familiality metric [Revelle, 2011].

Participant-level ICN consistency within task (split-half analysis)

To address the question of ICN consistency within task, each scan was divided into equal halves and the group-level ICNs from the meta-ICAs of each task were used as the templates in separate dual regressions performed on the

corresponding halved data sets (for HI and VG, respectively). The meta-ICA maps were used for these analyses to allow for interpretability of subsequent comparisons of these split-half data to other metrics. The resulting participant-level spatial maps and timecourses from the subsequent dual regressions were used for a split-half analysis of the consistency within task of the following three metrics described above: (i) spatial overlap, (ii) mean coherence, and (iii) the relationship to task during each scan.

To assess how much the participant-level spatial maps changed during the scan, Dice's similarity calculations were performed between ICN spatial maps generated from the two respective halves of each task. These coefficients were averaged across individuals per ICN and described as the *Spatial Overlap Consistency* within each task (HI and VG). For the *Mean Coherence Consistency*, mean intranetwork coherence was calculated for the participant-level spatial maps generated from the two halves of data, for each task respectively, as described above (Supporting Information Methods) and the reliability within each task was calculated using ICC's. The task EV vectors were also halved and each half was correlated with the ICN timecourses generated from the corresponding half of the scan data using the calculation described in the *ICN timecourse analyses* section. These task-relevant scores were then *z*-transformed and submitted to an ICC in the *ICN Relationship to Task Consistency* metric.

Participant-level ICN consistency across tasks (cross-task network correspondence)

Additional metrics were computed to assess the extent to which network characteristics were stable from one task condition to the other at the participant level. At the group level, 15 networks were matched across the two tasks based on at least a modest level of Dice similarity (Dice threshold, $s \geq 0.4$). First, ICN consistency was assessed by performing 3D spatial correlations of the amount of overlap between matched participant-level ICN maps (HI vs. VG). Second, the consistency of the ICN coherence across tasks was assessed by calculating ICC's of the mean intranetwork coherence scores generated for the matched task ICNs across all individuals. Third, the set of *z*-transformed correlations between the task timeline and the participant-level ICN timecourses, for each task, was then submitted to an ICC calculation to assess the stability of ICN task relevance across tasks in an individual.

RESULTS

Relationship to Canonical Brain Networks

Nonartifactual group-level networks generated from the separate ICAs of the first twin group and second twin group exhibited a high degree of similarity (Supporting Information Fig. 1). As a result, the group components from the HI and VG tasks that were produced from the meta-ICA of the first twin group were selected for use in all subsequent analyses. These two sets of group-level maps were consequently back transformed into participant-level component maps and timecourses for all participants and, hence, full twin pairs. By using maps derived from only the first twin group the analyses were not artificially inflated by genetic covariance.

In both the HI and the VG data, 17 out of the 30 components generated by the meta-ICA procedure were nonartifactual (Fig. 1a). Dice similarity coefficients calculated between these two sets of group-level ICN spatial maps highlighted a one-to-one or a one-to-two correspondence between the ICNs derived from the two tasks (Fig. 1b). The canonical networks from the BrainMap database (Laird et al., 2011) were subsequently correlated with each set of ICNs for comparison and reverse inference of function. This showed that there was a modest or good correspondence between each BrainMap network and an ICA derived-ICN (Fig. 2). To determine whether the ICNs derived from the different tasks were related to the BrainMap networks in a similar way, we tested the relationship between the group-level inference correlation scores (Table I, data columns 1 and 2). These were correlated at $r = 0.50$ ($P = 0.057$), indicating that the ICNs that were the best matches to the BrainMap networks could be consistent across the two tasks.

Relationship to Task

Timecourse analyses showed both strongly positive and strongly negative correlations between the ICN timecourses and the convolved HRF design matrix vectors for both tasks (Table I, columns 3 and 4). In all tests, significance testing with the effective sample size and Bonferroni correction were applied. For the HI task, the networks that had significant positive relationships to the task were the arm/hand sensorimotor network ($r = 0.82$), MT + MST/association visual network ($r = 0.81$), area V1/simple visual stimuli network ($r = 0.61$), and the visuospatial reasoning network ($r = 0.56$). Additionally, the subgenual cingulate cortex and orbitofrontal cortex network had a significant anticorrelation with the task timeline ($r = -0.56$). For the VG task, the networks that had significant positive relationships to the task were the area V1/simple visual stimuli network ($r = 0.70$) and left executive and language processing network ($r = 0.66$); no networks showed a significant anticorrelation with the task timeline. Taken together, these results show that the networks that were most engaged by each task were networks with functions relevant to the particular task demands, including visual processing of stimuli, sensorimotor processing for HI, and language processing for VG.

Participant-Level Network Consistency Within Task (Split-Half)

In the split-half analysis of ICN spatial overlap consistency, average Dice overlap scores ranged from $s = 0.64$ to

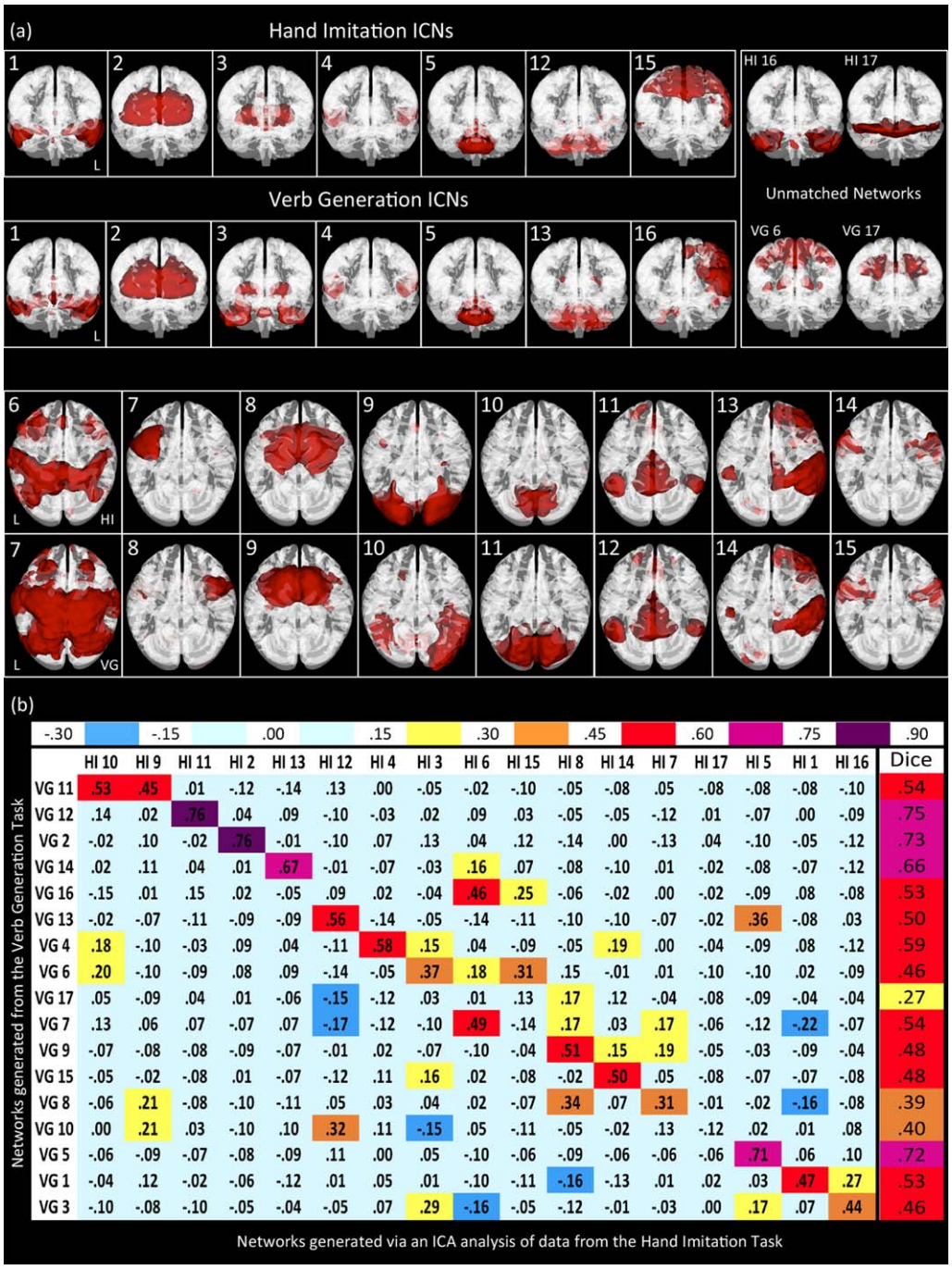

Figure 1.

Networks generated from the HI and VG tasks. (**a**) 3D overlays of ICNs were rendered in either coronal or axial orientations for the first two and last two rows, respectively. For each orientation, the HI ICNs are in the first row and the VG ICNs in the second. (**b**) Spearman rank-order correlations and Dice similarity correlations were calculated between ICN maps from the HI and VG tasks. These two sets of ICA-derived ICNs underwent spatial correlations with a threshold for at least a modest score on the Dice similarity index ($s \geq 0.4$). In addition, the Spearman correlations were found to be significant above a threshold of $r \geq 0.433$ at $\alpha < 0.05$. [Color figure can be viewed in the online issue, which is available at wileyonlinelibrary.com.]

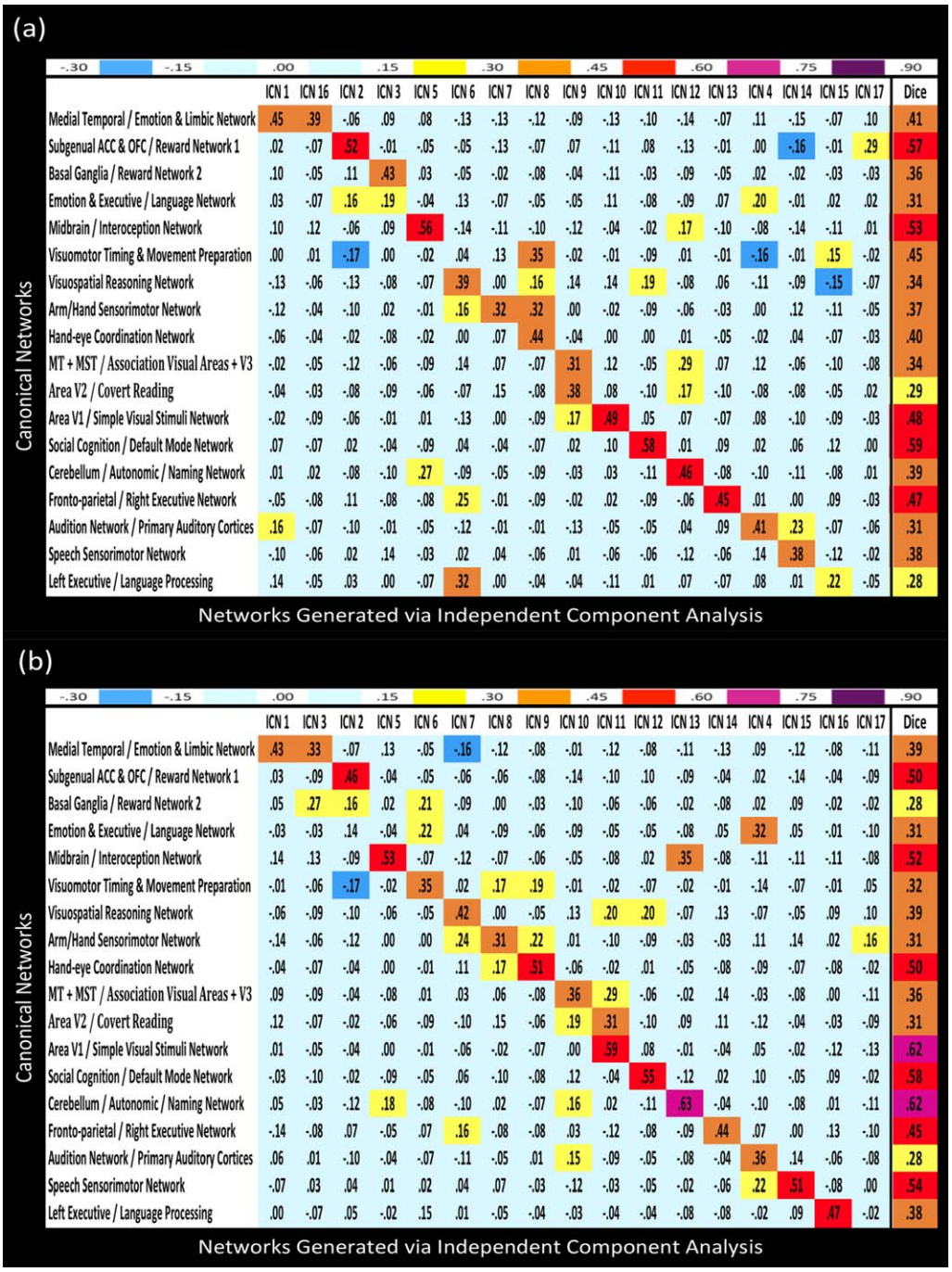

Figure 2.

Spearman rank-order correlations and Dice similarity correlations were calculated between the network masks from the BrainMap database and the ICN spatial maps generated from the ICA of functional data from (**a**) the HI task and (**b**) the VG task. ICA networks were assessed for having at least a modest score on the Dice similarity index ($s \geq 0.4$) with a corresponding BrainMap network. In addition, the Spearman correlations were found to be significant above a threshold of ($r \geq 0.433$) at $\alpha < 0.05$. [Color figure can be viewed in the online issue, which is available at wileyonlinelibrary.com.]

TABLE I. Summary statistics for reverse inference and the ICN relationships to the tasks

Network	Reverse Inference Component	Inference correlation		Relationship to Task	
		HI (90% Cl)	VG (90% Cl)	HI (95% Cl)	VG (95% Cl)
1	Medial temporal/Emotion & Limbic Network 1	**0.45** (0.10 0.70)	0.43 (0.00 0.73)	−0.24 (−0.32 −0.15)	0.24 (0.17 0.31)
2	Subgenual ACC & OFC/Reward 1a	**0.52** (0.19 0.75)	**0.46** (0.04 0.74)	**−0.56 *** (−0.63 −0.50)	−0.36 (−0.41 −0.30)
3	Basal Ganglia/Reward Network 2	**0.43** (0.07 0.69)	0.27 (−0.18 0.63)	0.03 (−0.07 0.13)	−0.10 (−0.15 −0.04)
4	Emotion & Executive/Language & Auditory Cortices	0.20 (−0.18 0.53)	0.36 (−0.08 0.69)	0.00 (−0.09 0.08)	−0.17 (−0.24 −0.11)
5	Midbrain/Interoception Network	**0.56** (0.24 0.77)	**0.53** (0.13 0.78)	0.05 (−0.05 0.15)	−0.05 (−0.10 0.00)
6	Visuospatial Reasoning Network	0.39 (0.02 0.66)	0.42 (−0.01 0.72)	**0.56 *** (0.49 0.61)	0.05 (−0.04 0.13)
7	Arm/Hand Sensorimotor Network	0.32 (−0.06 0.62)	0.31 (−0.14 0.65)	**0.82 *** (0.78 0.86)	−0.21 (−0.29 −0.13)
8	Hand-eye Coordination Network	**0.44** (0.08 0.70)	**0.51** (0.10 0.77)	0.00 (−0.09 0.08)	−0.17 (−0.24 −0.10)
9	MT + MST/Areas V2 & V3/Covert reading	0.38 (0.01 0.66)	0.36 (−0.08 0.69)	**0.81 *** (0.78 - 0.84)	−0.18 (−0.27 −0.09)
10	Area V1/Simple Visual Stimuli Network	**0.49** (0.15 0.73)	**0.59 *** (0.21 0.81)	**0.61 *** (0.54 - 0.70)	**0.70 *** (0.65 0.74)
11	Social Cognition/Default Mode Network	**0.58 *** (0.27 0.78)	**0.55** (0.16 0.79)	**−0.39** (−0.47 −0.31)	−0.35 (−0.44 −0.26)
12	Cerebellum/Autonomic/Naming Network	**0.46** **(0.11 0.71)**	**0.63 *** (0.27 0.83)	−0.20 (−0.31 −0.07)	0.21 (0.14 0.28)
13	Fronto-parietal/Right Executive Network	**0.45** (0.10 0.70)	**0.44** (0.01 0.73)	**−0.34** (−0.42 −0.26)	−0.15 (−0.23 −0.06)
14	Speech Sensorimotor Network	0.38 (0.01 0.66)	**0.51** (0.10 0.77)	−0.14 (−0.20 −0.08)	0.04 (−0.05 0.12)
15	Left Executive/Language Processing	0.22 (−0.16 0.55)	**0.47** (0.05 0.75)	**−0.39** (−0.47 −0.31)	**0.66 *** (0.59 0.71)
16	Medial temporal/Emotion 2	0.39 (0.02 0.66)		0.00 (−0.11 0.10)	
17	Subgenual ACC & OFC/Reward 1b	0.29 (−0.09 0.60)		−0.15 (−0.23 −0.06)	
18	Visuomotor Timing & Movement Preparation		0.35 (−0.10 0.68)		**0.44** (0.40 0.49)
19	Arm/Hand Sensorimotor Network 1b		0.16 (−0.29 0.55)		**−0.32** (−0.38 −0.27)

Note: *Reverse Inference Component* and *Inference Correlation*: Reverse Inference Component labels derived from Laird, et al., 2011 (http://fsl.fmrib.ox.ac.uk/analysis/brainmap+rsns/). *Relationship to Task*: mean correlations of the participant-level design matrix hemodynamic response function (HRF) with ICN timecourses. Network correlation scores were bolded at significance threshold of $p < 0.05$. Significant correlations that survived Bonferroni correction were starred ($p < 0.0029$). Some confidence intervals do not include zero, but the values were not found to be significant after adjustments with the effective sample size (see Methods). HI = hand imitation, VG = Verb Generation, CI = Confidence Interval.

$s = 0.90$ for the HI task, and from $s = 0.64$ to $s = 0.91$ for the VG task. For HI, the highest spatial consistency within-task was observed in the midbrain/interoception network ($s = 0.90$), followed by the default mode network (DMN) ($s = 0.86$), and the area V1/simple visual stimuli network ($s = 0.85$). For VG, the highest spatial overlap was observed in the area V1/simple visual stimuli network ($s = 0.91$), followed by the hand–eye coordination network ($s = 0.87$) and the DMN ($s = 0.86$). The overall consistency of the morphology of the ICNs during the task was excellent and comparable in both tasks ($s = 0.76$ for HI; $s = 0.74$ for VG) (Table II, data columns 1 and 2).

The ICC's from the split-half analysis of mean coherence consistency ranged from 0.19 to 0.75 for HI, and from 0.18 to 0.79 for VG. For HI, mean network coherence was most consistent within-task in the frontoparietal network (ICC

TABLE II. Participant-level ICN consistency within and across tasks

Mathched ntework #	Reverse inference componenet	Sapital overlap (Spilt Half - HI) (95% CI)	Sapital overlap (Spilt Half - VG) (95% CI)	Sapital overlap HI vs VG (95% Cl)	Mean coherence (Spilt Half - HI) (95% CI)	Mean coherence (Spilt Half - VG) (95% CI)	Mean coherence HI vs VG (95% CI)	Relationship to task (Spilt Half - HI) (95% CI)	Relationship to task (Spilt Half - VG) (95% CI)	Relationship to task HI vs VG (95% CI)
1	Medial temporal/Emotion & Limbic Network 1	0.65 (0.63 0.67)	0.64 (0.61 0.66)	0.49 (0.48 0.49)	0.31 (0.03 0.55)	0.66 (0.45 0.80)	0.47 (0.21 0.68)	0.69 (0.49 0.82)	0.40 (0.12 0.62)	0.08 (−0.07 0.29)
2	Subgenual ACC & OFC/Reward 1a	0.76 (0.73 0.80)	0.68 (0.64 0.72)	0.76 (0.75 0.77)	0.63 (0.41 0.78)	0.69 (0.48 0.82)	0.59 (0.36 0.76)	0.47 (0.19 0.67)	0.21 (−0.10 0.48)	0.25 (−0.06 0.52)
3	Basal Ganglia/Reward Network 2	0.83 (0.80 0.85)	0.68 (0.66 0.71)	0.26 (0.25 0.27)	0.54 (0.29 0.72)	0.55 (0.30 0.73)	0.33 (−0.10 0.64)	0.69 (0.48 0.82)	0.70 (0.50 0.82)	−0.08 (−0.34 0.21)
4	Emotion & Executive/Language & Auditory Cortices	0.69 (0.67 0.71)	0.72 (0.70 0.73)	0.55 (0.54 0.56)	0.51 (0.25 0.71)	0.53 (0.28 0.71)	0.57 (0.33 0.74)	0.61 (0.35 0.78)	0.50 (0.24 0.70)	−0.04 (−0.27 0.23)
5	Midbrain/Interoception Network	0.90 (0.89 0.92)	0.81 (0.79 0.83)	0.82 (0.82 0.83)	0.52 (0.26 0.71)	0.73 (0.55 0.84)	0.18 (−0.08 0.44)	0.64 (0.43 0.79)	0.48 (0.21 0.68)	0.10 (−0.18 0.38)
6	Visuospatial Reasoning Network	0.75 (0.74 0.77)	0.79 (0.77 0.81)	0.51 (0.50 0.51)	0.45 (0.18 0.66)	0.79 (0.64 0.88)	0.47 (0.21 0.68)	0.56 (0.31 0.74)	0.46 (0.18 0.67)	0.09 (−0.07 0.30)
7	Arm/Hand Sensorimotor Network	0.68 (0.67 0.70)	0.64 (0.61 0.66)	0.37 (0.36 0.37)	0.57 (0.25 0.77)	0.76 (0.58 0.86)	0.15 (−0.08 0.42)	0.88 (0.80 0.94)	0.37 (0.09 0.60)	0.01 (−0.02 0.06)
8	Hand-eye Coordination Network	0.83 (0.81 0.85)	0.87 (0.85 0.89)	0.49 (0.49 0.50)	0.47 (0.20 0.68)	0.64 (0.42 0.79)	0.50 (−0.02 0.76)	0.59 (0.35 0.75)	0.42 (0.14 0.63)	0.11 (−0.14 0.36)
9	MT + MST/Areas V2 & V3/ Covert reading	0.82 (0.80 0.83)	0.49 (0.46 0.52)	0.29 (0.28 0.29)	0.56 (0.31 0.74)	0.18 (−0.11 0.45)	0.10 (−0.05 0.34)	0.41 (0.13 0.63)	0.52 (0.23 0.71)	−0.03 (−0.06 0.08)
10	Area V1/Simple Visual Stimuli Network	0.85 (0.84 0.87)	0.91 (0.90 0.92)	0.65 (0.64 0.65)	0.64 (0.41 0.79)	0.68 (0.48 0.81)	0.57 (0.23 0.77)	0.59 (0.34 0.76)	0.68 (0.48 0.82)	0.61 (0.31 0.79)
11	Social Cognition/Default Mode Network	0.86 (0.84 0.87)	0.86 (0.85 0.88)	0.81 (0.80 0.81)	0.44 (0.15 0.65)	0.70 (0.48 0.83)	0.60 (0.36 0.76)	0.52 (0.27 0.71)	0.62 (0.37 0.78)	0.37 (0.07 0.60)
12	Cerebellum/Autonomic/Naming Network	0.64 (0.61 0.67)	0.78 (0.75 0.82)	0.39 (0.38 0.39)	0.51 (0.26 0.70)	0.70 (0.51 0.83)	0.56 (0.32 0.74)	0.72 (0.54 0.84)	0.58 (0.34 0.75)	0.08 (−0.10 0.29)
13	Fronto-parietal/Right Executive Network	0.73 (0.71 0.75)	0.75 (0.73 0.77)	0.65 (0.64 0.66)	0.75 (0.58 0.86)	0.76 (0.59 0.86)	0.77 (0.61 0.87)	0.40 (0.11 0.62)	0.31 (0.00 0.56)	0.25 (−0.03 0.50)
14	Speech Sensorimotor Network	0.65 (0.63 0.67)	0.76 (0.74 0.78)	0.31 (0.26 0.36)	0.19 (−0.11 0.46)	0.75 (0.59 0.86)	0.55 (0.30 0.73)	0.01 (−0.29 0.31)	0.36 (0.07 0.60)	0.33 (0.02 0.58)
15	Left Executive/Language Processing	0.75 (0.73 0.77)	0.73 (0.71 0.74)	0.27 (0.26 0.27)	0.53 (0.28 0.72)	0.55 (0.29 0.73)	0.50 (0.16 0.71)	0.60 (0.37 0.76)	0.51 (0.25 0.70)	−0.03 (−0.07 0.07)
	Average Across Networks	0.76	0.74	0.51	0.51	0.64	0.46	0.56	0.47	0.14

Note: *Spatial Overlap Consistency*: (a) for the split-half spatial overlap calculation, the participant-level ICN spatial maps generated from the two respective halves of each task were compared using Dice's similarity index and the similarity coefficients were averaged across individuals per ICN. (b) To assess the cross-task ICN spatial overlap (HI vs. VG), spatial maps of matched ICNs from the ICAs of the HI and VG tasks underwent a Dice similarity calculation at individual level and these similarity coefficients were averaged per ICN. *Mean Coherence Consistency*: (c) for the split-half coherence consistency, the mean coherence was calculated for the participant-level ICNs generated from each half (see methods) and the reliability within task was calculated using ICC's. (d) For the cross-task coherence consistency, ICC's were calculated using the two sets of participant-level mean coherence values for matched ICNs (HI vs. VG). *ICN Relationship to Task Consistency*: (e) in the split-half consistency calculation, the ICNs' relationships to the respective portions of the task was first established using a Pearson correlation and an ICC was then calculated of the z-transformed correlations scores for each half of the task. (f) In the cross-task "relationship to task" consistency metric (HI vs. VG), the two sets of participant-level correlations of the ICN timecourse and the task timeline in each task were z-transformed and these z-transformed values were correlated across matched ICNs. *Average Across Networks*: Overall score within each modality (column averages). HI = hand imitation, VG = Verb Generation, CI = Confidence Interval.

= 0.75), followed by the area V1/simple visual stimuli network (ICC = 0.64). For VG, mean network coherence was most consistent in the visuospatial reasoning network (ICC = 0.79), followed by the frontoparietal network (ICC = 0.76). The overall consistency of mean network coherence during the task was good for both tasks (ICC = 0.51 for HI; ICC = 0.64 for VG) (Table II, data columns 4 and 5).

The ICC's from the split-half analysis of *z*-transformed scores for the ICNs' relationship to task had a range of 0.01–0.88 for HI and 0.21–0.70 for VG. The task relevance of the ICNs was most consistent during the task for the arm/hand sensorimotor network (ICC = 0.88) for HI and the basal ganglia network for VG (ICC = 0.70). The overall consistency of the task relevance of the ICNs was found to be good and comparable in both tasks (ICC = 0.56 for HI; ICC = 0.47 for VG) (Table II, data columns 7 and 8).

Participant-Level Network Consistency Across Different Tasks (Cross-Task)

For the analysis of the correspondence of individual level spatial maps across tasks, it was found that the midbrain/interoception network had the highest participant-level spatial consistency (*s* = 0.82), followed by the DMN (*s* = 0.81) (Table II). Overall, the task-to-task spatial consistency across all individuals and matched networks was found to be 0.51 (Table II, data column 3). The frontoparietal/right executive network showed the highest consistency for mean coherence scores across the two tasks (ICC = 0.77), and the overall consistency of ICN coherence across tasks was 0.46 (Table II, data column 6). When looking at the consistency of each network's response to differential task demands (task relevance), ICN timecourses were most similar across tasks for the area V1/simple visual stimuli network (ICC = 0.61). However, owing to the fact that the ICNs showed differential task-relevant changes in their timecourses during each task, there was low overall consistency of ICN timecourses across tasks (ICC = 0.14) (Table II, data column 9), suggesting many of the ICNs were sensitive to specific aspects of task demands.

Task Familiality

Using the task HRF familiality metric, which assessed the degree to which twins showed similar relationships between the ICN timecourses and the task timeline, four ICNs showed significant correspondence within twin pairs after Bonferroni correction in the HI task (Table III, data column 1). These ICNs were the area V1/simple visual stimuli network (ICC = 0.63), the hand–eye coordination network (ICC = 0.59), the basal ganglia network (ICC = 0.49), and the emotion and executive network (ICC = 0.49). In the VG task, the networks that showed significant task HRF familiality after Bonferroni correction were the left executive/language processing network (ICC = 0.57), the visuomotor timing and movement preparation network (ICC = 0.57), the DMN (ICC = 0.48), and the arm/hand sensorimotor network (ICC = 0.48) (Table III, data column 2). Given that the levels of ICN task HRF familiality did not simply map onto the magnitude of task relevance in either task, this suggests that the familiality metric measured covariance in twins' brains over-and-above task relevance.

Spatial Familiality

The spatial overlap familiality metric was used to indicate the correspondence of twin scores for the extent of spatial overlap of individual-level ICN spatial maps with the group maps in each task. Of the networks that passed multivariate significance thresholds in the HI task, it was found that the basal ganglia reward network exhibited the highest familiality (ICC = 0.65), followed by the frontoparietal/right executive network (ICC = 0.61) and the midbrain interoception network (ICC = 0.49) (Table III, data column 3). In the VG analysis, significant familiality was observed in the arm/hand sensorimotor network 1b (ICC = 0.66), the emotion and executive network (ICC = 0.51), the midbrain/interoception network (ICC = 0.48), the area V1/simple visual stimuli network (ICC = 0.48), and the arm/hand sensorimotor network (ICC = 0.48) (Table III, data column 4).

Intranetwork Coherence Familiality

To assess coherence familiality, mean network coherence score of ICC's and voxelwise ICC's was calculated. There were several networks that were found to exhibit significant familiality for the mean network coherence analysis after corrections for multiple comparisons. For ICNs from the HI task, the ICN with significance that survived Bonferroni correction was the MT + MST/association visual network (ICC = 0.63) (Table III, data column 5). For ICNs from the VG task, the area V1/simple visual stimuli network exhibited the highest familiality (ICC = 0.68), followed by the frontoparietal/right executive network (ICC = 0.65), and the arm/hand sensorimotor network (ICC = 0.62) (Table III, data column 6). There was only a modest, nonsignificant correlation between the coherence familiality observed in each task (*r* = 0.30).

The magnitudes of the mean network coherence ICC's were two to three times the magnitude of the same metric when calculated voxel-by-voxel. For example, for HI task, the three highest voxelwise ICC scores were for the midbrain interoceptive network (ICC = 0.33), basal ganglia/reward network (ICC = 0.27), and area V1/simple visual stimuli network (ICC = 0.21), but none of these reached the level of significance (Supporting Information Fig. 2a). Similarly, for the VG task, the highest voxelwise ICC's were for the area V1/simple visual stimuli network (ICC = 0.31), midbrain interoceptive network (ICC = 0.28), and

cerebellar network associated with autonomic and naming tasks (ICC = 0.26), which were also nonsignificant (Supporting Information Fig. 2b). Interestingly, the area V1/simple visual stimuli network was found to be one of the networks with the highest familiality using both the mean network coherence and the voxelwise coherence metrics, which suggests that this network exhibits robust coherence familiality; however, it appeared that the network-level analyses amalgamate the signal more efficiently than voxelwise analyses.

Permutation Testing

After selecting the group components from the ICA, the back-transformed participant-level spatial maps were used to generate heatmaps showing spatial correlations across all participants (Fig. 3). This analysis provided a different way of looking at familiality as in this case, all study participants were compared to each other. Consequently, the twin scores could be compared within this larger sample to see if there were group mean differences between twins and unrelated individuals. In the resulting heatmap, the diagonal showed that twins tend to have scores that are higher with their co-twin, that is for the twin pair than for unrelated individuals. This observation was then validated by performing a *t*-test of the group of twin pair scores versus scores for unrelated participants and it was found that the correlations were significantly higher within the twin pair (diagonal elements) than for unrelated individuals (off-diagonal elements) (t = 6.6856, df = 21.455, and P = 5.765e − 07). In addition, this finding was confirmed by a nonparametric permutation test in which twin pair membership was randomly reassigned (t = 19.5595, P = 3.373e − 13). Overall, these tests recapitulated that the ICNs exhibited a significant degree of familiality.

DISCUSSION

To examine the consistency and familiality of ICNs, we examined ICN phenotypes during two functional localizer tasks performed by 21 monozygotic twin pairs. These analyses revealed (1) common ICN characteristics that (2) showed a great degree of participant-level reproducibility within and across tasks, but were nevertheless (3) modulated to some degree by changes in task demands. (4) Several features showed significant familiality, including the extent to which brain networks were modulated by task demands, intranetwork coherence, and network morphology.

Relationship Between Canonical Brain Networks and Tasks

There was at least a modest Dice correlation, with strong one-to-one mappings, between the data-driven, group-level ICNs from the analyses of the HI and VG tasks, as well as between the ICNs from each task and the BrainMap networks. As such, this study is a validation of the functional associations from the BrainMap meta-analyses using raw data from task scans [Laird et al., 2011; for replication see Wisner et al., 2013] and shows that the meta-ICA algorithm was robust and captured generally the same networks from two highly dissimilar tasks. Furthermore, as a congruent set of networks was present in very different ICBM tasks, the findings of this study are evidence that a large proportion of the ICNs were not specific to a particular task. These results are consistent with previous studies that have shown that ICNs are not stimulus dependent, as similar networks have been derived during task and rest [Arbabshirani et al., 2012; Calhoun et al., 2008], as well as from an extensive task activation meta-analysis and resting state scans [Laird et al., 2011; Smith et al., 2009]. However, given that the ICNs from each task in this study were not identical, with some showing greater disparity compared to others, it remains to be determined how much of this results from systematic task-dependent variation versus instabilities in measurement and processing. Nevertheless, this study serves as a proof of principle that complements of brain networks can be captured under different circumstances, and that the same general network can be examined across varying contexts to examine how it changes.

Another goal of these analyses was to show that not only could canonical ICNs be derived from various behavioral paradigms, but also that the ICA algorithms would be sensitive to task manipulations in a manner that is complementary to traditional fMRI activation studies. In doing so, this study provides a separate, additional validation of the BrainMap functional associations by not only using the spatial correspondence of activation networks and ICNs, but also employing direct analysis of raw fMRI data and the resulting ICN timecourses. Consequently, task relevance was established for networks with meta-analytical functional associations to hand motions in the HI task, including a network with premotor areas that are putative mirror neuron regions, as well as for language-related networks in the VG task. These functionally relevant ICNs were not only selectively and significantly related to separate tasks using timecourse analyses, but they also contained regions that had been previously reported to be related to these tasks in traditional GLM paradigms. Within the HI task, this is true for the visuospatial reasoning ICN, which contained the superior parietal lobe and ventral premotor cortex, as well as the association visual ICN, which contained the extrastriate visual cortex, and finally the network which encapsulated the primary visual cortex (area V1). The arm/hand sensorimotor ICN contained the hand regions of the pre- and postcentral gyri, and all of these areas contained within the ICNs have previously been found to be related to hand imitation [Grafton and Hamilton, 2007; Iacoboni, 2005; Jackson et al., 2006; Koski et al., 2003]. The same was true for the left executive and language processing ICN that was

TABLE III. Summary Statistics for ICN Familiality

Network	Reverse inference component	Task HRF familiality HI (95% CI)	Task HRF familiality VG (95% CI)	Spatial familiality HI (95% CI)	Spatial familiality VG (95% CI)	Coherence familiality HI (95% CI)	Coherence familiality VG (95% CI)
1	Medial temporal/Emotion & Limbic Network 1	0.01 (−0.44 0.45)	0.24 (−0.21 0.61)	0.37 (−0.07 0.68)	0.31 (−0.13 0.65)	0.37 (−0.07 0.69)	**0.44** (0.01 0.73)
2	Subgenual ACC & OFC/Reward 1a	0.20 (−0.25 0.58)	**0.38** (−0.03 0.69)	0.25 (−0.17 0.60)	**0.46** * (0.05 0.73)	0.20 (−0.27 0.58)	0.40 (−0.04 0.71)
3	Basal Ganglia/Reward Network 2	**0.49** * (0.07 0.76)	0.14 (−0.27 0.53)	**0.65** * (0.30 0.85)	0.38 (−0.04 0.69)	**0.50** (0.08 0.76)	**0.51** (0.11 0.77)
4	Emotion & Executive/Language & Auditory Cortices	**0.49** * (0.10 0.75)s	**0.46** (0.04 0.74)	0.17 (−0.29 0.56)	**0.51** * (0.10 0.77)	0.28 (−0.17 0.63)	0.43 (0.01 0.72)
5	Midbrain/Interoception Network	**0.39** (−0.04 0.69)	0.12 (−0.31 0.52)	**0.49** * (0.02 0.77)	**0.48** * (0.06 0.75)	**0.51** (0.10 0.80)	**0.57** (0.18 0.80)
6	Visuospatial Reasoning Network	0.00 (−0.42 0.42)	**0.43** (0.00 0.72)	0.14 (−0.26 0.51)	**0.43** (0.02 0.72)	0.19 (−0.28 0.57)	**0.55** (0.17 0.79)
7	Arm/Hand Sensorimotor Network	−0.11 (−0.53 0.34)	**0.48** * (0.08 0.75)	**0.41** (−0.01 0.71)	**0.48** * (0.05 0.76)	**0.48** (0.06 0.75)	**0.62** * (0.27 0.83)
8	Hand-eye Coordination Network	**0.59** * (0.27 0.83)	0.14 (−0.21 0.49)	0.06 (−0.40 0.48)	0.35 (−0.09 0.67)	−0.04 (−0.48 0.40)	**0.47** (0.04 0.74)
9	MT + MST/Areas V2 & V3/Covert reading	−0.10 (0.07 0.76)	0.02 (−0.44 0.45)	0.29 (−0.11 0.63)	0.08 (−0.38 0.49)	**0.63** * (0.29 0.83)	**0.54** (0.17 0.78)
10	Area V1/Simple Visual Stimuli Network	**0.63** * (0.27 0.83)	**0.40** (−0.02 0.70)	0.17 (−0.22 0.54)	**0.48** * (0.08 0.75)	**0.54** (0.14 0.78)	**0.68** * (0.37 0.86)
11	Social Cognition/Default Mode Network	**0.43** (0.00 0.72)	**0.48** * (0.07 0.76)	0.16 (−0.28 0.55)	0.30 (−0.10 0.63)	**0.50** (0.09 0.76)	0.40 (−0.03 0.70)
12	Cerebellum/Autonomic/Naming Network	**0.42** (−0.01 0.72)	0.34 (−0.10 0.67)	0.18 (−0.21 0.54)	0.08 (−0.31 0.46)	0.07 (−0.35 0.47)	**0.53** (0.13 0.78)
13	Fronto-parietal/Right Executive Network	0.16 (−0.31 0.55)	**0.45** (0.04 0.73)	**0.61** * (0.24 0.82)	0.26 (−0.16 0.61)	0.39 (−0.05 0.70)	**0.65** * (0.31 0.84)
14	Speech Sensorimotor Network	−0.07 (−0.44 0.63)	0.28 0.34) (−0.17	**0.38** (−0.01 0.68)	−0.06 (−0.49 0.38)	0.36 (−0.08 0.68)	0.34 (−0.11 0.67)
15	Left Executive/Language Processing	0.12 (−0.35 0.52)	**0.57** * (0.21 0.80)	−0.01 (−0.46 0.43)	0.21 (−0.20 0.57)	0.27 (−0.18 0.63)	0.15 (−0.32 0.55)
16	Medial temporal/Emotion 2	0.11 (−0.34 0.51)		**0.40** (0.00 0.70)		0.13 (−0.31 0.53)	
17	Subgenual ACC & OFC/Reward 1b	0.19 (−0.28 0.57)		**0.45** (0.04 0.73)		0.17 (−0.28 0.55)	
18	Visuomotor Timing & Movement Preparation	**0.57** * (0.21 0.80)			0.19 (−0.28 0.57)		0.22 (−0.22 0.59)
19	Arm/Hand Sensorimotor Network 1b	0.07 (−0.32 0.46)			**0.66** * (0.32 0.85)		0.40 (−0.04 0.71)

Note. *Task HRF Familiality*: cross-twin correlation of z-transformed scores of task correlation coefficients; *Spatial Familiality*: cross-twin correlation of z-transformed scores of correspondence between individual and group level maps; *Coherence Familiality*: cross-twin ICC of individuals' average coherence scores. Network correlation scores were bolded at an uncorrected significance threshold of $p < 0.05$. Significant correlations that survived Bonferroni correction were starred ($p < 0.0029$).

significantly related to the VG task timeline as it contained both Broca's and Wernice's areas, which have been heavily associated with verb generation [Crivello et al., 1995; Edwards et al., 2010; Indefrey, 2011; Indefrey and Levelt, 2004].

These findings lend credence to the assertion that the data are not overfit, and that this ICA method can be used to examine task manipulations [Calhoun et al., 2001]. These ICNs reflect the activity of real, relevant brain regions and the ICA method used to produce them can provide information about which networks receive even subtle perturbations from the task presentation, which might not be captured by a typical GLM subtraction paradigm. Hence, it is apparent that this new approach can provide information that is complementary to activation paradigms [Smith, 2012]. However, any claims can only be made about the relevance of ICN modulation by these two tasks. Hence, future studies will directly relate the results of a traditional GLM to an ICA in the same task data set to determine the extent to which this is a general principle.

The arm/hand sensorimotor and visuospatial reasoning networks were strongly related to the task timeline of the HI task, but the hand–eye coordination network was not related at all. There are several explanations for this curious finding, including that the participants were lying supine in the scanner and, as such, were not looking at their hands and not making parabolic, grasping, or other complex actions that might have engaged the hand–eye coordination network. A similar finding is that in the analysis of the VG task, the left executive and language processing network, which includes both Broca's and Wernice's areas, was significantly related to the task, but the speech sensorimotor network and the composite network associated with emotion and executive functioning, language, and the primary auditory cortices did not exhibit strong task relevance. In the case of the VG task, the participants were instructed to look at a picture and generate a verb or action without actually speaking it out loud. Hence, it is likely that the task engaged the left executive and language processing network as well as visuomotor timing and movement preparation network, but not the speech sensorimotor network as there was no verbal output and associated activity in that part of the motor cortex. Similarly, as the participants were producing no sounds, it is reasonable that the auditory network was also not engaged by the task in a significant manner.

Another observation is that both the DMN and the executive networks were anticorrelated with the task. This at first seemed counterintuitive as executive networks are typically described as being antagonistic to the DMN [Fox and Raichle, 2007; Raichle et al., 2001]. However, the control condition is a passive monitoring task, which the DMN has been shown to be involved in [Greicius and Krasnow, 2003; Li et al., 2012]. Additionally, this monitoring task probably recruited the executive networks more than the task condition owing to the need for sustained vigilance for the particular arrow that required a button-press response, in contrast to the HI and VG tasks that elicited more stereotyped responses.

Within-Task and Cross-Task Consistency

In general, it was found that ICNs have good to excellent consistency within tasks regardless of the metric used. For the spatial overlap split-half consistency, the midbrain and DMNICNs consistently had some of the highest scores in both the HI and the VG tasks. Hence, it is not surprising that this results in these two networks having the highest scores for the crosstask reproducibility of the spatial maps. This observation also holds for the area V1/simple visual stimuli network as it also had one of the highest levels of spatial reproducibility and mean coherence for the split-half analyses and, subsequently, the crosstask analysis. Although there are other networks that had high scores in the morphology and coherence analyses as well, when considering the relationship to task, area V1 had good reliability in both tasks for the split-half analyses and a comparable score for the crosstask analysis, which was almost twice the magnitude as the next highest ICNs, making the consistency of task relevance in V1 a unique finding.

The previous studies, such as Zuo et al. (2010) have employed test–retest reliability measures to ICA data and they found that the networks with the highest within-participant reproducibility were their medial visual network, frontoparietal networks, DMN, and executive control network. In a later study, Wisner et al. (2013) found that group-level reproducibility was highest for the V1/simple visual stimuli network, followed by the DMN. In addition, when comparing the ICN group maps from their test–retest and crossvalidation samples with BrainMap networks, the simple visual stimuli network showed the highest level of consistent spatial overlap [Wisner et al., 2013]. These findings are supported by those of this study which shows that the area V1/simple visual stimuli network emerges as the ICN with the best consistency. Hence, V1 had the highest average rank (and group of averages) for the consistency metrics, both within each task and across tasks. This is likely owing to the fact that V1 is a unimodal input area that has a stereotyped response, and this will be discussed further below.

In general, the three methods of assessing the consistency of ICNs provided evidence that the morphology and coherence of the ICNs showed good overall consistency, both within and across tasks. However, although the relationship with task was stable within each task, this metric exhibited low consistency across tasks, which implies that the dynamics of a functional network when engaged in different tasks are stable but divergent and the ICA therefore captures context-dependent variability in ICN

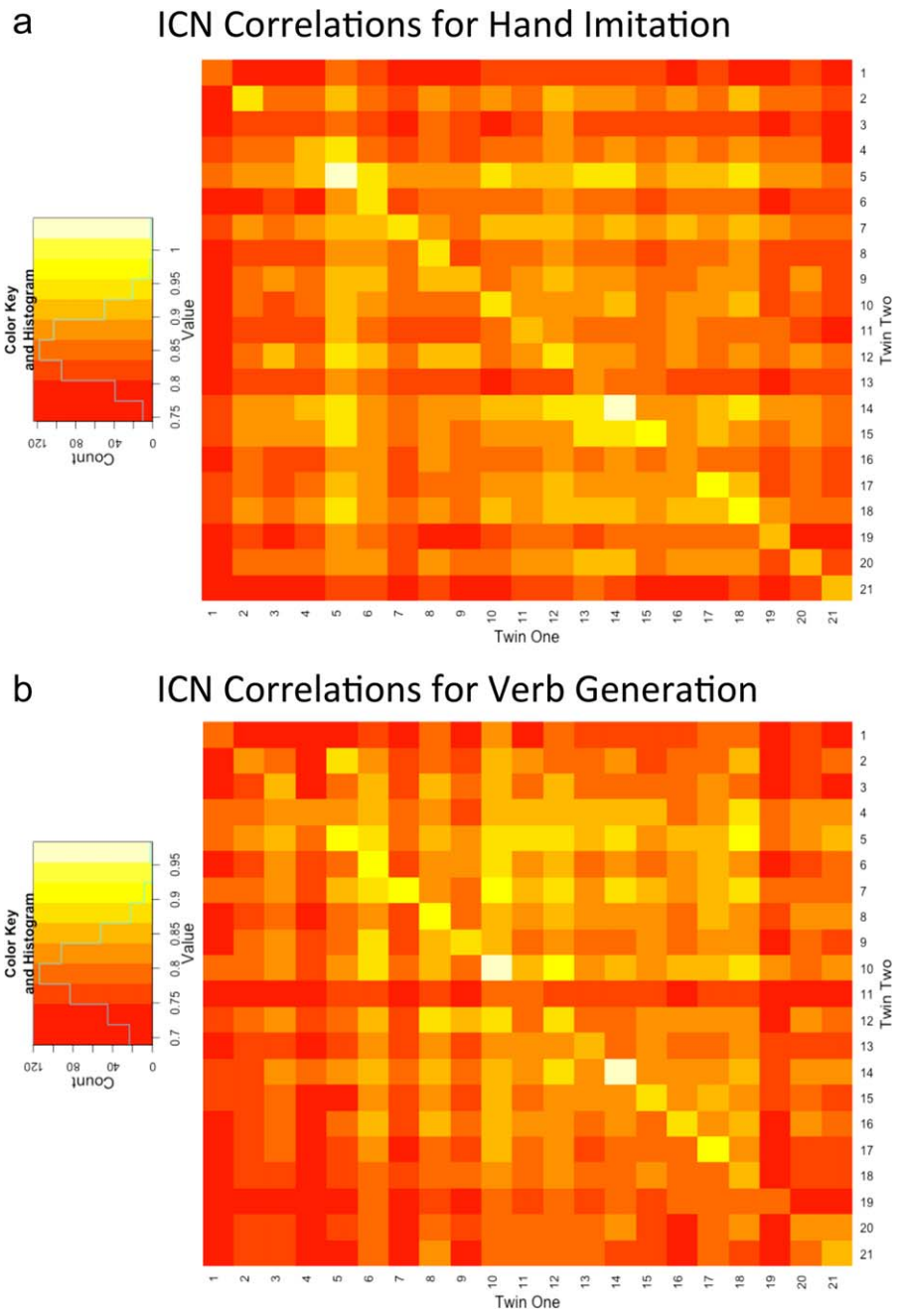

Figure 3.

Heatmaps showing spatial correlations across all participants averaged across all ICNs. The correlations for each twin with their co-twin lie on the diagonal and the correlations with all other unrelated individuals can be found in the corresponding row or column. Correlation scores ranged from 0 to 1 and the scores for each task are represented in a 21 × 21 matrix. [Color figure can be viewed in the online issue, which is available at wileyonlinelibrary.com.]

timecourses. In addition, the characteristics of these ICNs being relatively stable within and across tasks, with the exception of divergent task relevance, are supported by the findings that show that there is a correspondence between network states during a task and at rest [Calhoun et al., 2008; Hampson and Driesen, 2006; Hermundstad et al., 2013; Li et al., 2013]. Hence, our findings are in line with the assertion that the brain is typically in a

multistable state that is optimized and primed for different forms of either endogenous or exogenous activity [Deco and Corbetta, 2012]. Given that stable functional connectivity architecture has been reported across many studies, which include task paradigms, these results support the notion that the introduction of a task does not override the baseline state in the brain [Arfanakis et al., 2000; Biswal et al., 2010; Fox and Raichle, 2007].

Familiality

Given that there are several networks that are significantly related to task but that do not show task HRF timecourse familiality and vice versa, the results of this study suggest that the familiality of network timecourses is not solely dependent on how those network timecourses are being modulated or driven by the task timeline. Similarly, familiality does not appear to be a function of split-half or crosstask consistency. This is significant as it shows that the observed familiality is not simply a reflection of how well captured or stable the network is, nor is it based on how regularized the signal is because it is being driven by task presentation. However, future work is needed to determine the upper and lower bounds of reliability and task influence on heritability estimates. Hence, the same methods need to be applied to the data in a great variety of paradigms to determine if there are networks that are both strongly heritable and consistently impervious to task modulation.

Nevertheless, the present findings support a notable level of familiality worth investigating further. The heatmaps of ICN correlations show a clear diagonal, which indicates that the highest (hottest) scores were those between cotwins and the *t*-test and permutation test validated the significance of this finding. In particular, the area V1/simple visual stimuli network was not only familial, but also significantly related to task in both the HI and the VG paradigms, and showed strong consistency within and across tasks in all three domains (V1 was prominent in almost all analyses). Hence, it is possible that the primary visual cortex is the most robust marker of functional connectivity as it was well captured by the ICA, could be modulated by exogenous activity, but also preserved a level of consistency, as well as genetic covariance in its morphology, timecourse, and coherence.

It is interesting that area V1 was one of the networks that exhibited the most robust network consistency and heritability estimates, given the recent observation that interparticipant variability in internetwork coherence is lowest in visual areas and highest in frontoparietal networks [Mueller et al., 2013]. These authors argue that individual differences in internetwork connectivity are related to the phylogenetic development of brain structures, which makes variability highest in multimodal association cortex areas, but lowest in unimodal sensory regions. One way to contextualize these findings is to note that although it is true that having zero variability precludes the observation of any familiality, high interparticipant variability does not automatically imply familiality, as other studies have found that there is an increase in discordance in certain brain regions and functions in twins over time and experience [Lessov-Schlaggar et al., 2012; Wallace et al., 2006]. In addition, it has been shown that brain activity in visual areas is heritable, which implies that if the reduction of variability in sensorimotor regions means that they are less sensitive to nongenetic influences, instead of driving down familiality this would actually boost familiality [Park et al., 2012].

Limitations

One relevant aspect of this discussion that these results could not directly assess is the proportion of covariance in twins that might be attributable to shared environment as the participants were all monozygotic twins and no dizygotic twins were recruited for this study. In addition, although the sample size is comparable to other fMRI twin studies, this study is underpowered when compared to larger behavioral genetic heritability models. Finally, we administered only two tasks and this limits the generalizability of the results. In the HI and VG paradigms, the participants could not be rated on how well they were performing the tasks and, as a result, we cannot infer how ICN consistency or familiality was reflected in behavior. Hence, future study will need to be done to include tasks in many more domains, including tasks that have measurable behavioral output.

CONCLUSIONS

This study advances the current understanding of the trait-like nature of ICN-based metrics pertaining to task relevance, consistency, and familiality. In this study, monozygotic twins completed two dissimilar and stereotypical tasks that were designed to produce activation in discrete brain regions by using stimuli that would drive activity in specific brain networks. Hence, these tasks have an identical design and periodicity and share an identical button press "off" state, but they are quite different in their cognitive demands. As a result, they have provided a useful means for exploring and contrasting the ways in which exogenous demands can affect the characteristics of ICNs. We found that the ICA-derived ICNs detected across two different task states were stable across time within each task, highly similar in their morphology and coherence across tasks, and their timecourses reflected task-dependent modulation selectivity in networks with functional relevance to each task. Based on the present analyses, it appears that the extent to which an ICN is driven by the task does not determine its familiality, but rather this familiality seems to be selectively expressed and its detection may be

somewhat limited by the network's consistency. Taken together, these results suggest that it is possible that the familiality of ICNs is related to the variability or complexity of the underlying neuronal architecture, but more work needs to be done to further establish and explore this principle.

ACKNOWLEDGMENTS

Preliminary results from this study were presented at the 19th annual meeting of the Cognitive Neuroscience Society in Chicago, Illinois. Data collection for this study was supported through a National Alliance for Research on Schizophrenia and Depression young investigator award to A. W. MacDonald. The authors are grateful to Roger Woods, who provided the stimuli and parameters for the two paradigms, and to Andrew Poppe and Edward Patzelt who provided analytical tools and advice.

REFERENCES

Agresti A (2013): Categorical Data Analysis, 3rd ed. Hoboken, New Jersey: Wiley Series on Probability and Statistics.

Ambrosius U, Lietzenmaier S, Wehrle R, Wichniak A, Kalus S, Winkelmann J, Friess E (2008). Heritability of sleep electroencephalogram. Biol Psychiatr 64:44–48.

Anderson J, Ferguson MA, Lopez-Larson M, Yurgelun-Todd D (2011): Reproducibility of single-subject functional connectivity measurements. Am J Neuroradiol 32:548–555.

Andersson JLR, Jenkinson M, Smith S (2007): Non-linear registration, aka spatial normalisation. Oxford Centre for Functional MRI of the Brain Technical Report TR07JA2.

Arbabshirani MR, Havlicek M, Kiehl KA, Pearlson GD, Calhoun VD (2012): Functional network connectivity during rest and task conditions: A comparative study. Hum Brain Mapp. 34: 2959–2971.

Arfanakis K, Cordes D, Haughton VM, Moritz CH, Quigley MA, Meyerand ME (2000): Combining independent component analysis and correlation analysis to probe interregional connectivity in fMRI task activation datasets. Magn Reson Imaging 18:921–930. Retrieved from http://www.ncbi.nlm.nih.gov/pubmed/11121694.

Banerjee M, Capozzoli M, Mcsweeney L, Sinha D (2012): Beyond kappa: A review of interrater agreement measures. Can J Stat 27:3–23.

Beckmann CF (2012): Modelling with independent components. Neuroimage 62:891–901.

Beckmann C, Smith S (2004): Probabilistic independent component analysis for functional magnetic resonance imaging. Inst Elect Electron Eng Trans Med Imaging 23:137–152. Retrieved from http://ieeexplore.ieee.org/xpls/abs_all.jsp?arnumber=1263605.

Behrens TEJ, Sporns O (2011): Human connectomics. Curr Opin Neurobiol 22:1–10.

Belmonte MK, Carper RA (2006): Monozygotic twins with Asperger syndrome: Differences in behaviour reflect variations in brain structure and function. Brain Cognit 61:110–121.

Bhaganagarapu K, Jackson GD, Abbott DF (2013): An automated method for identifying artifact in independent component analysis of resting-state fMRI. Front Hum Neurosci Methods 7:1–17.

Biswal B, Eldreth D, Motes M, Rypma B (2010): Task-dependent individual differences in prefrontal connectivity. Cereb Cortex 4:1–10.

Biswal B, Mennes M, Zuo XN, Gohel S, Kelly C, Smith SM, Beckmann CF, Adelstein JS, Buckner RL, Colcombe S, Dogonowski AM, Ernst M, Fair D, Hampson M, Hoptman MJ, Hyde JS, Kiviniemi VJ, Kötter R, Li SJ, Lin CP, Lowe MJ, Mackay C, Madden DJ, Madsen KH, Margulies DS, Mayberg HS, McMahon K, Monk CS, Mostofsky SH, Nagel BJ, Pekar JJ, Peltier SJ, Petersen SE, Riedl V, Rombouts SA, Rypma B, Schlaggar BL, Schmidt S, Seidler RD, Siegle GJ, Sorg C, Teng GJ, Veijola J, Villringer A, Walter M, Wang L, Weng XC, Whitfield-Gabrieli S, Williamson P, Windischberger C, Zang YF, Zhang HY, Castellanos FX, Milham MP (2010): Toward discovery science of human brain function. Proc Natl Acad Sci USA 107:4734–4739.

Blokland GAM, McMahon KL, Hoffman J, Zhu G, Meredith M, Martin NG, Thompson PM, de Zubicaray GI, Wright MJ (2008): Quantifying the heritability of task-related brain activation and performance during the N-back working memory task: A twin fMRI study. Biol Psychol 79:70–79.

Blokland GAM, McMahon KL, Thompson PM, Martin NG, de Zubicaray GI, Wright MJ (2011): Heritability of working memory brain activation. J Neurosci 31:10882–10890.

Borgwardt SJ, Picchioni MM, Ettinger U, Toulopoulou T, Murray R, McGuire PK (2010): Regional gray matter volume in monozygotic twins concordant and discordant for schizophrenia. Biol Psychiatry 67:956–964.

Brun C, Leporé N, Pennec X, Lee A, Barysheva M, Madsen SK, Avedissian C, Chou YY, de Zubicaray GI, McMahon KL, Wright MJ, Toga AW, Thompson PM (2009): Mapping the regional influence of genetics on brain structure variability—A tensor-based morphometry study. Neuroimage 48:37–49.

Calhoun V, Adali T (2001): A method for making group inferences from functional MRI data using independent component analysis. Hum Brain Mapp 151:140–151.

Calhoun VD, Adali T, Mcginty VB, Pekar JJ, Watson TD, Pearlson GD (2001): fMRI activation in a visual-perception task: Network of areas detected using the general linear model and independent components analysis. Neuroimage 14:1080–1088.

Calhoun V, Kiehl K, Pearlson G (2008): Modulation of temporally coherent brain networks estimated using ICA at rest and during cognitive tasks. Hum Brain Mapp 29:828–838.

Calhoun VD, Liu J, Adali T (2009): A review of group ICA for fMRI data and ICA for joint inference of imaging, genetic, and ERP data. Neuroimage 45:S163–S172.

Chen C-H, Gutierrez ED, Thompson W, Panizzon MS, Jernigan TL, Eyler LT, Fennema-Notestine C, Jak AJ, Neale MC, Franz CE, Lyons MJ, Grant MD, Fischl B, Seidman LJ, Tsuang MT, Kremen WS, Dale AM (2012): Hierarchical genetic organization of human cortical surface area. Science 335:1634–1636.

Chiang M-C, McMahon KL, de Zubicaray GI, Martin NG, Hickie I, Toga AW, Wright MJ, Thompson PM (2011): Genetics of white matter development: A DTI study of 705 twins and their siblings aged 12 to 29. Neuroimage 54:2308–2317.

Chou Y, Panych L, Dickey CC, Petrella JR, Chen N (2012): Investigation of long-term reproducibility of intrinsic connectivity network mapping: A resting-state fMRI study. Am J Neuroradiol 33:833–838.

Crivello F, Tzourio N, Poline J, Woods RP, Mazziotta JC, Mazoyer B (1995): Intersubject variability in functional neuroanatomy of silent verb generation: Assessment by a new activation

detection algorithm based on amplitude and size information.pdf. Neuroimage 2:253–263.

Deco G, Corbetta M (2012): The dynamical balance of the brain at rest. Neuroscientist 17:107–123.

Deco G, Jirsa V, Mcintosh AR, Sporns O, Ko R (2009): Key role of coupling, delay, and noise in resting brain fluctuations. Proc Natl Acad Sci USA 106:10302–10307.

Deco G, Jirsa VK, McIntosh AR (2011): Emerging concepts for the dynamical organization of resting-state activity in the brain. Nat Rev Neurosci 12:43–56.

Duarte-Carvajalino JM, Jahanshad N, Lenglet C, McMahon KL, de Zubicaray GI, Martin NG, Wright MJ, Thompson PM, Sapiro, G (2012): Hierarchical topological network analysis of anatomical human brain connectivity and differences related to sex and kinship. Neuroimage 59:3784–3804.

Edwards E, Nagarajan S, Dalal S (2010): Spatiotemporal imaging of cortical activation during verb generation and picture naming. Neuroimage 50:291–301.

Fornito A, Bullmore E (2012): Connectomic intermediate phenotypes for psychiatric disorders. Front Psychiatry 3:1–15.

Fox MD, Raichle ME (2007): Spontaneous fluctuations in brain activity observed with functional magnetic resonance imaging. Nat Rev Neurosci 8:700–711.

Glahn DC, Winkler AM, Kochunov P, Almasy L, Duggirala R, Carless MA, Curran JC, Olvera RL, Laird AR, Smith SM, Beckmann CF, Fox PT, Blangero J (2010): Genetic control over the resting brain. Proc Natl Acad Sci USA 107:1223–1228.

Grafton ST, Hamilton AFDC. (2007). Evidence for a distributed hierarchy of action representation in the brain. Hum Mov Sci 26:590–616.

Greicius M, Krasnow B (2003): Functional connectivity in the resting brain: A network analysis of the default mode hypothesis. Proc Natl Acad Sci USA 100:253–258.

Greicius M, Kiviniemi V, Tervonen O, Vainionpää V, Alahuhta S, Reiss AL, Menon V (2008): Persistent default-mode network connectivity during light sedation. Hum Brain Mapp 29:839–847.

Guo CC, Kurth F, Zhou J, Mayer EA, Eickhoff SB, Kramer JH, Seeley WW (2012): Neuroimage one-year test—Retest reliability of intrinsic connectivity network fMRI in older adults. Neuroimage 61:1471–1483.

Hagmann P, Cammoun L, Gigandet X, Gerhard S, Grant PE, Wedeen V, Meuli R, Thiran JP, Honey CJ, Sporns O (2010): MR connectomics: Principles and challenges. J Neurosci Methods 194:34–45.

Hallmayer J, Cleveland S, Torres A, Phillips J, Cohen B, Torigoe T, Miller J, Fedele A, Collins J, Smith K, Lotspeich L, Croen LA, Ozonoff S, Lajonchere C, Grether JK, Risch N (2011): Genetic heritability and shared environmental factors among twin pairs with autism. Arch Gen Psychiatry 68:1095–1102.

Hampson M, Driesen N (2006): Brain connectivity related to working memory performance. J Neurosci 26:13338–13343.

Hermundstad AM, Bassett DS, Brown KS, Aminoff EM, Clewett D, Freeman S, Frithsen A, Johnson A, Tipper CM, Miller MB, Grafton ST, Carlson JM (2013): Structural foundations of resting-state and task-based functional connectivity in the human brain. Proc Natl Acad Sci USA 110:6169–6174.

Honey CJ, Thivierge J-P, Sporns O (2010): Can structure predict function in the human brain? Neuroimage 52:766–776.

Hothorn T, Hornik K (2011): ExactRankTests: Exact distributions for rank and permutation tests. R Package Version 0.8-22. Retrieved from http://cran.r-project.org/package=xactRankTests.

Iacoboni M (2005): Neural mechanisms of imitation. Curr Opin Neurobiol 15:632–637.

Indefrey P (2011): The spatial and temporal signatures of word production components: A critical update. Front Psychol 2:1–16.

Indefrey P, Levelt WJM (2004): The spatial and temporal signatures of word production components. Cognition 92:101–144.

Jackson PL, Meltzoff AN, Decety J (2006): Neural circuits involved in imitation and perspective-taking. Neuroimage 31:429–439.

Jahanshad N, Lee AD, Barysheva M, McMahon KL, de Zubicaray GI, Martin NG, Wright MJ, Toga AW, Thompson, PM (2010): Genetic influences on brain asymmetry: A DTI study of 374 twins and siblings. Neuroimage 52:455–469.

Jang JH, Jung WH, Choi JS, Choi CH, Kang DH, Shin NY, Hong KS, Kwon JS (2011): Reduced prefrontal functional connectivity in the default mode network is related to greater psychopathology in subjects with high genetic loading for schizophrenia. Schizophr Res 127:58–65.

Jenkinson M, Bannister P, Brady M, Smith S (2002): Improved optimization for the robust and accurate linear registration and motion correction of brain images. Neuroimage 17:825–841.

Koski L, Iacoboni M, Dubeau M, Woods RP, John C (2003): Modulation of cortical activity during different imitative behaviors modulation of cortical activity during different imitative behaviors. J Neurophysiol 89:460–471.

Kristo G, Rutten G-J, Raemaekers M, de Gelder B, Rombouts S, Ramsey N (2012): Task and task-free FMRI reproducibility comparison for motor network identification. Hum Brain Mapp. 35:340–352.

Lahaye P, Poline J, Flandin G (2003): Functional connectivity: Studying nonlinear, delayed interactions between BOLD signals. Neuroimage 20:962–974.

Laird AR, Fox PM, Eickhoff SB, Turner JA, Ray KL, McKay DR, Glahn DC, Beckmann CF, Smith SM, Fox PT (2011): Behavioral interpretations of intrinsic connectivity networks. J Cogn Neurosci. 23:4022–40371. Retrieved from http://www.hubmed.org/display.cgi?uids=21671731.

Lessov-Schlaggar C, Hardin J, DeCarli C, Krasnow RE, Reed T, Wolf PA, Swan GE, Carmelli D (2012): Longitudinal genetic analysis of brain volumes in normal elderly male twins. Neurobiol Aging 33:636–644.

Li B, Wang X, Yao S, Hu D, Friston K (2012): Task-dependent modulation of effective connectivity within the default mode network. Front Psychol 3:1–11.

Li N, Ma N, Liu Y, He X-S, Sun D-L, Fu X-M, Zhang X, Han SZhang D-R (2013): Resting-state functional connectivity predicts impulsivity in economic decision-making. J Neurosci 33: 4886–4895.

Matthews SC, Simmons AN, Strigo I, Jang K, Stein MB, Paulus MP (2007): Heritability of anterior cingulate response to conflict: An fMRI study in female twins. Neuroimage 38:223–227.

Mazziotta J, Toga A, Evans A, Fox P, Lancaster J, Zilles K, Mazoyer B (2001): A probabilistic atlas and reference system for the human brain: International Consortium for Brain Mapping (ICBM). Philos Trans R Soc Lond B Biol Sci 356:1293–1322.

Mazziotta JC, Woods R, Iacoboni M, Sicotte N, Yaden K, Tran M, Bean C, Kaplan J, Toga AW; Members of the International Consortium for Brain Mapping (ICBM) (2009): The myth of the normal, average human brain—The ICBM experience: (1) subject screening and eligibility. Neuroimage 44:914–922.

Mckeown MJ, Makeig S, Brown GG, Jung T, Kindermann SS, Bell AJ, Sejnowski TJ (1998): Analysis of fMRI data by blind

separation into independent spatial components. Hum Brain Mapp 6:160–188.

Meier T, Wildenberg J, Liu J, Chen J (2012): Parallel ICA identifies sub-components of resting state networks that covary with behavioral indices. Front Hum Neurosci 6:1–14.

Meyer-Lindenberg A (2009): Neural connectivity as an intermediate phenotype: Brain networks under genetic control. Hum Brain Mapp 30:1938–1946.

Molloy E, Blumenthal J, Giedd JN, Liu H, Jeffriest N, Zijdenboss A, Rapoport JL (2001): The relationship between brain morphometry and cognitive abilities in healthy pediatric monozygotic twins. Neuroimage 13, S447.

Mueller S, Wang D, Fox MD, Yeo BTT, Sepulcre J, Sabuncu MR, Shafee R, Lu J, Liu H (2013): Individual variability in functional connectivity architecture of the human brain. Neuron 77: 585–595.

Munn MA, Alexopoulos J, Nishino T, Babb CM, Flake LA, Singer T, Ratnanather JT, Huang H, Todd RD, Miller MI, Botteron KN (2007): Amygdala volume analysis in female twins with major depression. Biol Psychiatry 62:415–422.

Park J, Shedden K, Polk TA (2012): Correlation and heritability in neuroimaging datasets: A spatial decomposition approach with application to an fMRI study of twins. Neuroimage 59: 1132–1142.

de Pasquale F, Della Penna S, Snyder AZ, Marzetti L, Pizzella V, Romani GL, Corbetta M (2012): A cortical core for dynamic integration of functional networks in the resting human brain. Neuron 74:753–764.

Pedlow S, Wang Y, Muircheartaigh CO (2005): The impact of cluster (segment) size on effective sample size. Paper Presented at the 60th Annual Meeting of the American Association For Public Opinion Association, Fontainebleau Resort, Miami Beach, FL. Retrieved from http://www.allacademic.com/meta/p17146_index.html.

Poppe AB, Wisner K, Atluri G, Lim KO, Kumar V, Macdonald AW (2013): Toward a neurometric foundation for probabilistic independent component analysis of fMRI data. Cogn Affect Behav Neuroscience. 13:641–659.

Raichle ME, MacLeod AM, Snyder AZ, Powers WJ, Gusnard DA, Shulman GL (2001): A default mode of brain function. Proc Natl Acad Sci USA 98:676–682.

Ray KL, Mckay DR, Fox PM, Riedel MC, Uecker AM, Beckmann CF, Smith SM, Fox PT, Laird AR (2013): ICA model order selection of task co-activation networks. Front Neurosci 7:1–12.

Repovš G, Barch D (2012): Working memory related brain network connectivity in individuals with schizophrenia and their siblings. Front Hum Neurosci 6:1–15.

Revelle W (2011): psych: procedures for personality and psychological research Northwestern University, Evanston. R Package Version 1.01.9.

Rimol LM, Panizzon MS, Fennema-Notestine C, Eyler LT, Fischl B, Franz CE, Hagler DJ, Lyons MJ, Neale MC, Pacheco J, Perry ME, Schmitt JE, Grant MD, Seidman LJ, Thermenos HW, Tsuang MT, Eisen SA, Kremen WS, Dale AM (2010): Cortical thickness is influenced by regionally specific genetic factors. Biol Psychiatry 67:493–499.

Sämann PG, Wehrle R, Hoehn D, Spoormaker VI, Peters H, Tully C, Holsboer F, Czisch M (2011): Development of the brain's default mode network from wakefulness to slow wave sleep. Cereb Cortex 21:2082–2093.

Shehzad Z, Kelly AMC, Reiss PT, Gee DG, Gotimer K, Uddin LQ, Lee SH, Margulies DS, Roy AK, Biswal BB, Petkova E, Castellanos FX, Milham, MP (2009): The resting brain: Unconstrained yet reliable. Cereb Cortex 19:2209–2229.

Smith S, Fox P, Millera KL, Glahn DC, Fox PM, Mackay CE, Filippini N, Watkins KE, Toro R, Laird AR, Beckmann CF (2009): Correspondence of the brain's functional architecture during activation and rest. Proc Natl Acad Sci USA 106:13040–13045. Retrieved from http://www.pnas.org/content/106/31/13040.short.

Smith SM (2012): The future of FMRI connectivity. Neuroimage 62:1257–1266.

Snyder AZ, Raichle ME (2012): A brief history of the resting state: The Washington University perspective. Neuroimage 62:902–910.

Tarokh L, Carskadon MA, Achermann P (2011): Trait-like characteristics of the sleep EEG across adolescent development. J Neurosci 31:6371–6378.

Thomason M, Dennis E, Joshi A (2011): Resting-state fMRI can reliably map neural networks in children. Neuroimage 55:650–670.

Tost H, Bilek E, Meyer-Lindenberg A (2011): Brain connectivity in psychiatric imaging genetics. Neuroimage 62:2250–2260.

Van Dijk KRA, Hedden T, Venkataraman A, Evans KC, Lazar SW, Buckner RL (2010): Intrinsic functional connectivity as a tool for human connectomics: Theory, properties, and optimization. J Neurophysiol 103:297–321.

Wallace GL, Eric Schmitt J, Lenroot R, Viding E, Ordaz S, Rosenthal MA, Molloy EA, Clasen LS, Kendler KS, Neale MC, Giedd JN (2006): A pediatric twin study of brain morphometry. J Child Psychol Psychiatry Allied Discip 47:987–993.

Wisner KM, Atluri G, Lim KO, Iii AWM (2013): Neurometrics of intrinsic connectivity networks at rest using fMRI: Retest reliability and cross-validation using a meta-level method. Neuroimage 76:236–251.

Yang Y, Remmers EF, Ogunwole CB, Kastner DL, Gregersen PK, Li W (2011): Effective sample size: Quick estimation of the effect of related samples in genetic case-control association analyses. Comput Biol Chem 35:40–49.

Yang Y, Joshi A, Joshi S, Baker L, Narr KL, Raine A, Thompson PM, Damasio H (2012): Genetic and environmental influences on cortical thickness among 14-year-old twins. Neuroreport 23: 702–706.

Zuo X, Kelly C, Adelstein JS, Klein DF, Castellanos FX, Milham MP (2010): Reliable intrinsic connectivity networks: Test–retest evaluation using ICA and dual regression approach. Neuroimage 49:2163–2177.